Raman spectroscopy evidence of inhomogeneous disorder in the bismuth-oxygen framework of $Bi_{25}InO_{39}$ and other sillenites

D. J. Arenas,[1] Theo Jegorel,[1,2] Chris Knab,[1] L. V. Gasparov,[1] C. Martin,[3] Daniel M. Pajerowski,[4] Hideo Kohno,[5] and Michael W. Lufaso[6]

[1]*Department of Physics, University of North Florida, Jacksonville, Florida 32224, USA*

[2]*Laboratoire de Nanotechnologie et d'Instrumentation Optique - UMR CNRS 6279, Universitẽ Technologie de Troyes, 12 rue Marie Curie, Troyes 10010, France*

[3]*Department of Physics, University of Florida, Gainesville, Florida 32611, USA*

[4]*NIST Center for Neutron Research, Gaithersburg, Maryland 20899, United States*

[5]*Department of Physics, Graduate School of Science, Osaka University, 1-1 Machikaneyama, Toyonaka, Osaka 560-0043, Japan*

[6]*Department of Chemistry, University of North Florida, Jacksonville, Florida 32224, USA*

(Received 21 May 2012; revised manuscript received 25 September 2012; published 26 October 2012)

We report the room-temperature Raman spectra of polycrystalline $Bi_{25}InO_{39}$ for the first time along with the spectrum of $Bi_{25}FeO_{39}$. Both samples were synthesized by the conventional solid state method. The spectra of these compounds are remarkably similar to each other and those of other sillenites. A comparison of these sillenites, and others reported in the literature, shows that the Bi-O modes soften for compounds with larger (ionic radii) M cations. The widths of the modes increase for the compounds with larger M cations: the increase in width is attributed to inhomogeneous disorder in deviations of the Bi-O bond lengths across different unit cells. The results show that large M cations affect the Bi-O framework around the tetrahedron. The parameters of each Raman mode were obtained by fitting the spectral lines to a Lorentzian oscillator model, and the modes were assigned to symmetry-allowed vibrations of the *I*23 space group.

DOI: 10.1103/PhysRevB.86.144116 PACS number(s): 78.30.−j

I. INTRODUCTION

The sillenite structure has been researched for technologically interesting photorefractive,[1–3] piezoelectric,[4] electro-optic,[5–7] and elasto-optic properties.[8,9] Sillenites continue to be relevant in the materials science community and have been the focus of recent first principles,[10,11] magnetism,[12] and high-pressure studies.[13,14] New sillenites with various M cations and dopants continue to be synthesized and studied to improve the photorefractive and electro-optic properties.[5,15–17]

The sillenite structure belongs to the cubic space group *I*23, No. 197. The structure is a Bi-O framework that connects MO_4 tetrahedra (see Fig. 1). The four oxygens in the tetrahedra are generally labeled as O(3), the oxygen atoms in the diagonals of the unit cell O(2), and the oxygens placed in the lowest-symmetry positions O(1).[18] The importance of the M cation in the sillenite structure can be explained by its parent compound γ-Bi_2O_3, a metastable compound where 80% of the M positions are filled with Bi^{3+} ions and 20% are vacant. The introduction of M cations stabilizes the structure by replacing the Bi^{3+} ions at the centers of the tetrahedra and filling the vacancies. The ideal structure is held for the tetravalent cations $M = Ge^{4+}$, Si^{4+}, which is confirmed by neutron-scattering data on $Bi_{12}GeO_{20}$ and $Bi_{12}SiO_{20}$ that show a 100% occupancy of both tetrahedral and oxygen positions.[20,21] $Bi_{12}TiO_{20}$ is another heavily studied compound and, stoichiometrically, it should have a 100% occupancy on the M and oxygen positions; however, its neutron-scattering data shows that the occupancy of the tetrahedral position is 0.9 while the O(3) position is 0.97, and the deficiency is explained by the higher ionic radii of Ti^{4+} compared to Si^{4+} and Ge^{4+}.[20] For other valences, the centers of the tetrahedra are shared with Bi^{3+} to ensure charge balance. For example, M^{2+} cations occupy 1/3 of the M positions while Bi^{3+} cations fill the rest.[19] It should be pointed out that this structural point of view represented by Valant and Suvorov[19] is different from other authors who had previously reported Bi^{5+} ions in the tetrahedral position.[21,22] The description of the stoichiometry by Valant and Suvorov will be used during this paper.

Raman spectroscopy is useful in the study of sillenites. The Raman spectrum acts as a fingerprint of the sillenite structure in studies where bismuth oxides are doped and grown in many different conditions and yield different phases.[23–28] For the hexavalent M cations W^{6+} and Mo^{6+}, Raman spectra have been presented as evidence of the existence of the sillenite structure after previous authors had postulated the impossibility of these compounds.[24,25] The Raman spectrum is so sensitive with regard to the sillenite structure that it can pinpoint the optimal growth parameters in different grown techniques for powders or thin films.[28–30] Also, Raman spectroscopy can be a powerful addition to x-ray diffraction (XRD) measurements for compounds containing a range of elemental weights, where diffraction by heavier atoms swamps that by lighter atoms, such as in the sillenites.

This paper has two major purposes. First, we report the Raman spectra of $Bi_{25}InO_{39}$ and $Bi_{25}FeO_{39}$ polycrystalline samples grown by the conventional solid state method. The spectra from both samples are almost identical and the sillenite structure is confirmed by comparison to the spectra of other sillenites. The Raman bands were assigned to symmetry-allowed vibrations. Second and most importantly, we observe inhomogeneous disorder of the Bi-O framework for sillenites with large M cations. Large increases in the Raman line widths indicate a random distribution of force constants in the Bi-O bonds. The distribution of force constants, attributed to differing Bi-O bond lengths across different unit cells, is an indication of inhomogeneous disorder. Also, a

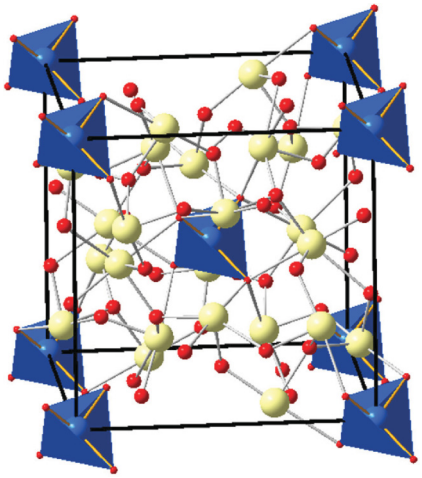

FIG. 1. (Color online) Sillenite structure. The structure is stabilized from the parent compound by an M cation in the center of the tetrahedra (i.e., Si^{4+}, Ti^{4+}, Fe^{3+}, In^{3+}). The tetrahedra (blue) at the corners and center of the unit cell are connected by BiO polyhedra that can be referred to as a Bi-O framework (Bi: yellow, O: red). There are three symmetry positions for oxygens: the O(3) oxygens form the corners of the tetrahedra while the O(1) and O(2) oxygens lie outside. More detail about the structure can be found in Refs. 18 and 19.

frequency-comparison of the most pronounced Raman bands shows that the force constants between the Bi, O(1) and O(2) atoms are decreased for compounds with large ionic radii. The wider and softer Raman modes show that large M cation distorts not only the tetrahedron but also the Bi-O framework outside it. The effect can be easily patterned against the ionic radius of the M site and may be useful in the study of new sillenites and/or new synthesis methods.

II. EXPERIMENTAL PROCEDURES

$Bi_{25}InO_{39}$ and $Bi_{25}FeO_{39}$ samples were synthesized by solid-state reaction in air using stoichiometrically weighed high purity oxides. Reactants were ground using an agate mortar and pestle under acetone, then initially heated at 700 °C in a high-form alumina crucible. Multiple heating cycles, with intermediate grinding, were conducted at 750 °C. Samples were analyzed by x-ray powder diffraction using a Rigaku Ultima III x-ray diffractometer with Cu Kα radiation. Equilibrium was assumed when no shift or change in intensity of the weakest peaks from the XRD pattern was observed. The structures of the single phase compounds were refined using the Rietveld technique and the FULLPROF software program. Scanning electron images (see Fig. 2) were taken using a JEOL JSM5510 SEM. Crystallites in the order of 10 μm were detected for both samples. We also synthesized $Bi_{25}GaO_{39}$, $Bi_{12}TiO_{20}$, $Bi_{12}GeO_{20}$, and $Bi_{12}SiO_{20}$ for comparison purposes.

Room-temperature Raman spectra were measured with a T 64000 Jobin Yvon triple Raman spectrometer equipped with a liquid-nitrogen-cooled back-illuminated CCD detector. We used the 514-nm line of the Ar^+ ion laser in a back-scattering geometry with an accumulation time of 16 seconds. The measurements were done in the subtractive mode[31] with a laser power not exceeding 1 mW focused to a 2-μm diameter. Both the scattered and the incident light had vertical polarization.

III. RESULTS AND DISCUSSION

A. Analysis of the Raman spectra

The room temperature spectra for $Bi_{25}FeO_{39}$ and $Bi_{25}InO_{39}$ are shown in Fig. 3. The spectra of $Bi_{12}SiO_{20}$, $Bi_{12}GeO_{20}$, $Bi_{12}TiO_{20}$, and $Bi_{25}GaO_{39}$, synthesized with the same method, are shown for comparison. To improve the analysis of each mode, most importantly at low frequencies, the imaginary part of the Raman susceptibility $\chi''(\omega)$ was obtained by correcting for the Bose factor of the Raman scattering cross section. The procedure is outlined in Ref. 33. To study each mode, we assumed a simple Lorentzian oscillator model for the susceptibility:

$$\chi(\omega) = \sum_{j}^{n} \frac{S_j^2}{\left(\omega_{oj}^2 - \omega^2\right) - i\omega\gamma_j}, \qquad (1)$$

where S_j^2 is the oscillator strength of each oscillator (related to the number of phonons involved in the vibration), while ω_{0j} and γ_j are the center frequency and damping coefficient of each oscillator, respectively. The physical advantage of this model is that the damping coefficient γ_j is the inverse of the lifetime of the electron occupying the j vibrational state, and therefore could be compared to an IR spectrum if this mode

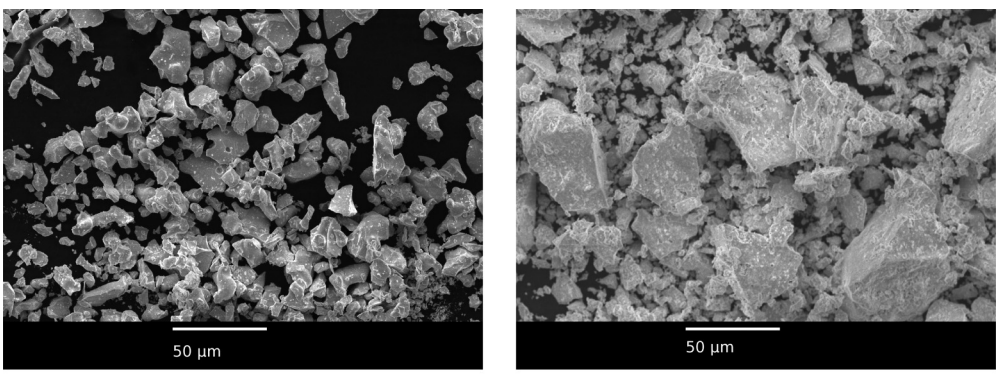

(a) $Bi_{25}InO_{39}$ (b) $Bi_{25}FeO_{39}$

FIG. 2. SEM images. Crystallites in the order of 10 microns were obtained for both samples using the conventional solid state method.

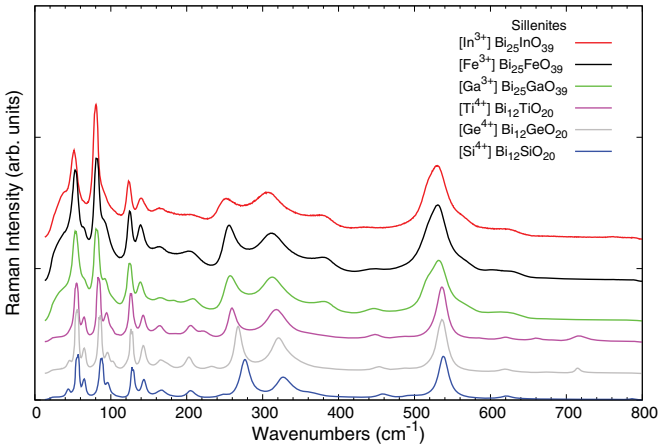

FIG. 3. (Color online) From top to bottom: Raman spectra of $Bi_{25}InO_{39}$ (red), $Bi_{25}FeO_{39}$ (black), $Bi_{25}GaO_{39}$ (green), $Bi_{12}TiO_{20}$ (magenta), $Bi_{12}GeO_{20}$ (gray), and $Bi_{12}SiO_{20}$ (blue). We synthesized and measured $Bi_{12}SiO_{20}$, $Bi_{12}GeO_{20}$, $Bi_{12}TiO_{20}$, and $Bi_{25}GaO_{39}$ for comparison. Details on the spectra of these four compounds have been presented elsewhere.[32] All spectra were scaled and shifted to ease comparison.

is both IR and Raman-active. However, the IR and Raman comparison of the damping coefficients may be difficult if other modes are overlapping. More details on this type of analysis is outlined in Ref. 33. Figure 4 shows the results for the imaginary susceptibilities in both samples, the fit to Eq. (1), and the individual oscillators used in the fit. Table I shows the parameters obtained from the Lorentzian oscillator model.

B. Comparison of Raman spectra and overall assignment of modes

The sillenite structure belongs to the cubic space group $I23$ and its factor-group analysis yields 40 optical modes:

$$\Gamma = 8A(R) + 8E(R) + 24F(R, IR) + F, \qquad (2)$$

where one F mode is acoustic, all modes are Raman-active (R) and only the F modes are IR active (IR). The Raman spectra of both samples display less than 15 modes. This is similar to other sillenites where not all 40 modes are resolved.[32,34] The Raman bands were assigned by comparison to other sillenites.[18,32,34,35] The assignments are possible due to detailed polarization measurements on single crystals of $Bi_{12}SiO_{20}$ and $Bi_{12}GeO_{20}$ by Ramdas *et al.*[35] and dynamical calculations by Mihailova[20,22] and Wojdowski.[18] Table II lists the frequencies of the Raman modes for our samples and others from the literature. The results show that most of the modes of $Bi_{25}InO_{39}$ and $Bi_{25}FeO_{39}$ have frequencies near those of other sillenites and confirm that these samples were successfully synthesized in the sillenite structure. The only major difference between the two compounds is a very weak mode around 770 cm^{-1} in $Bi_{25}InO_{39}$ that is not observed in $Bi_{25}FeO_{39}$. The absence of this band in one of the samples is not surprising since this mode is very weak in most samples and it is not observed in others.[22,32,35]

C. Relating the Raman spectra to the Bi-O framework

Calculations by Mihailova *et al.*[20,22] and Wojdowski *et al.*[18,20,22] give insight into the physical significance of the Raman modes. Table I shows the assignment of our spectra based on their calculations. The six strongest and most pronounced peaks of the Raman spectra (55, 85, 125, 260, 320, and 535 cm^{-1}) belong to vibrations involving Bi, O(1), and O(2). These modes are due to the Bi-O framework. Across different sillenites the Bi, O(1), and O(2) atoms are the same; therefore changes in the frequencies of these six Raman modes are related to differences in force constants inside the Bi-O framework. In fact, based on the assignments by Mihailova *et al.*,[20,22] most of the modes observed in the Raman spectra belong to the Bi-O framework and vibrations from the tetrahedra are better studied with infrared spectroscopy.[18,36] The following subsections have an extensive comparison of

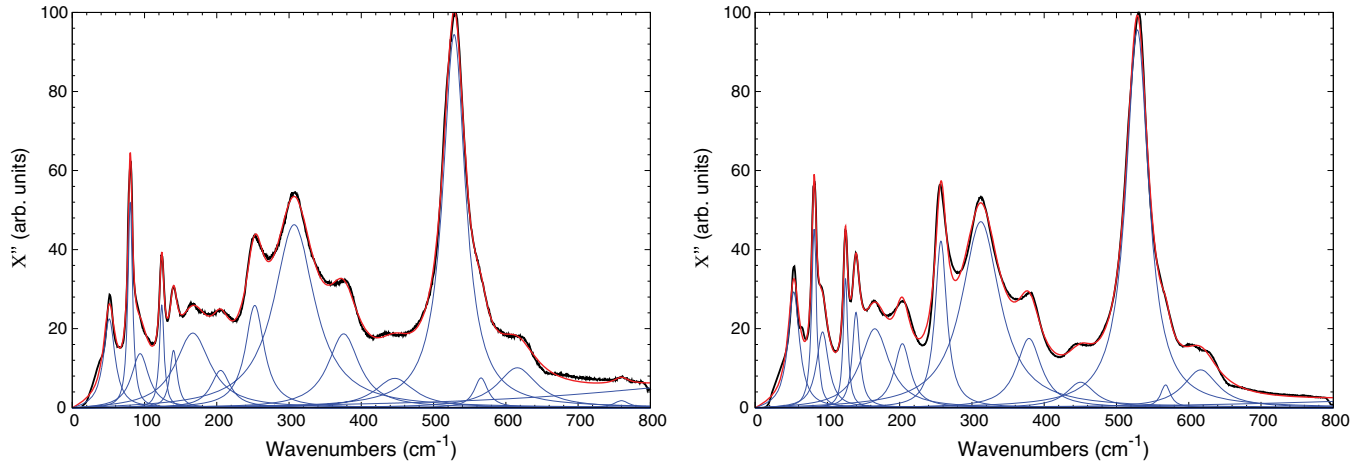

(a) $Bi_{25}InO_{39}$ (b) $Bi_{25}FeO_{39}$

FIG. 4. (Color online) Raman spectra corrected by a Bose factor for our two samples. The obtained imaginary part of the Raman susceptibility was fitted to a sum of Lorentzian oscillators: $\chi''(\omega) = [S_j^2\,\omega\,\gamma_j] / [(\omega_{oj}^2 - \omega^2)^2 + \omega^2\gamma_j^2]$. The figure shows the data (black), the fitting (red), and the individual functions (blue) from the fit. An arbitrary broad oscillator was added around 950 cm^{-1} to account for higher frequency contributions and background.

TABLE I. Parameters for $Bi_{25}InO_{39}$ and $Bi_{25}FeO_{39}$ from the Lorentzian oscillator model: $\chi''(\omega) = [S_j^2\,\omega\,\gamma_j] / [(\omega_{oj}^2 - \omega^2)^2 + \omega^2\gamma_j^2]$. The standard deviation of multiple measurements is around $\pm$ 1 cm^{-1} for the center frequency and $\pm$10% for the widths and amplitudes. Notice the strong similarities in many of the modes.

$Bi_{25}InO_{39}$			$Bi_{25}FeO_{39}$		
Strength S_j^2 (arb. u.)	ω_{oj} (cm^{-1})	γ_j (cm^{-1})	Strength S_j^2 (arb. u.)	ω_{oj} (cm^{-1})	γ_j (cm^{-1})
1.2	52	19	1.6	54	19
1.7	80	8	1.5	82	8
2.0	95	29	1.9	94	20
1.3	124	8	1.6	125	7
3.0	140	12	2.2	140	12
9.9	169	59	8.4	167	48
3.3	206	32	4.7	204	27
11	253	31	11	257	19
52	309	68	49	314	64
20	377	52	15	380	42
12	447	66	7.3	451	48
100	529	38	100	529	38
5.2	566	23	2.8	568	16
22	616	66	18	617	59
1.8	760	25	...	...	...

the six most pronounced Raman modes across the sillenites that were found in the literature. The six modes reveal that the Bi-O framework is affected by the M cation inside the tetrahedron.

1. *Valence of the M cation*

Complementary experimental evidence on the valence of cations is useful for synthetic chemists and crystallographers. In Table II, most of the Raman modes of $Bi_{25}InO_{39}$ and $Bi_{25}FeO_{39}$ are generally at lower frequencies than those of the tetravalent compounds. To see if this pattern applies to all sillenites, the Raman modes frequencies were plotted in Fig. 5 versus the valence of the M cation for our samples and those found in the literature. Only the frequency of the six most pronounced peaks in the spectra were plotted (these six modes are also considered strong or very strong by other references). The weak and broad modes are harder to compare due to inherent uncertainty in center frequency. In Fig. 5, the tetravalent compounds are $Bi_{12}SiO_{20}$, $Bi_{12}GeO_{20}$, and $Bi_{12}TiO_{20}$.[13,14,20,22,32,34,35,37–40] Complex compounds, such as $Bi_{36}MgP_2O_{60}$ and $Bi_{24}AlPO_{40}$,[34,41] are plotted using the average valence. Only sillenites with appreciable concentrations of M cations are considered here; reports of $Bi_{12}SiO_{20}$ and $Bi_{12}TiO_{20}$ doped with many different atoms but with small dopant concentrations[20,39,42] were not relevant in this comparison. The trivalent compounds are B^{3+},[27] In^{3+}, Fe^{3+}, and Ga^{3+}. The divalent cations are Zn^{2+} and Pb^{2+}.[26,32,34] The only pentavalent cation shown is V^{5+} and there are two hexavalent cations for Mo^{6+} and W^{6+}.[23–25] We offer an extensive comparison to encompass many different synthesis methods and measurement procedures. Over 40 Raman spectra were used from over 20 different references. Si^{4+} has the largest number of data points including crystals grown by the Czochralski method,[13,14,22,37–39] thin films,[29,40] powders,[32] and nanocrystals.[28,30] For some compounds, such as Zn, we were able to plot data from both crystals and powders.[32,34] In Fig. 5, the high-frequency outliers belong mostly to low-temperature studies of silicon, germanium, and titanium data.

There is a statistically significant difference between the Raman frequencies of the tetravalent cations and the lower valences. There is no significant difference for the higher valences, but the comparison is weaker since only three Raman spectra were found and the low-frequency part was not reported in these three compounds.

TABLE II. Comparison of the Raman modes of $Bi_{25}InO_{39}$ and $Bi_{25}FeO_{39}$ to other bismuth sillenites. The assignments were made based on the polarization measurements of single crystals of $Bi_{12}SiO_{20}$ and $Bi_{12}GeO_{20}$ by Ramdas *et al.*[35] and the lattice dynamical calculations by Mihailova[20,22] and Wojdowski.[18] The most pronounced modes of the sillenite structure are marked with † (these are the modes studied in Figs. 5–10).

Raman frequencies (cm^{-1})								
					Ref. 32		Ref. 32	
Si^{4+}	Ge^{4+}	Ti^{4+}	Ga^{3+}	Fe^{3+}	Zn^{2+}	In^{3+}	Pb^{2+}	Mode assignment[18,20,22,35]
56	56	55	55	54	51	52	50	F: Bi, O(1), and O(2) vibrations†
88	86	84	82	82	80	80	78	E: Bi, O(2) and O(3) vibrations elongating the cluster†
98	96	95	94	94				A: Libration of Bi-O(1) bonds and breathing of O(2) atoms
129	127	126	125	125	126	124	132	E: Bi and O(2) vibrations along [100] or [010]†
144	143	143	140	140	139	140	145	A: Breathing of Bi and O(2) atoms
167	168	164	172	167	166	169	164	F: Breathing of Bi and all O atoms
205	203	206	207	204		206		F: Bi-O(2) and Bi-O(1) modes
277	268	261	259	257	253	253	251	E: O(2) breathing and weak Bi-O(1) rocking†
328	322	319	315	314	310	309	317	A: Bi-O(1) rocking and weak O(2) breathing†
351		369	380	380	373	377		F: O(1)-Bi-O(2) and O(1)-Bi-O(3) bending?
458	453	450	448	451		447		E: Tetrahedral mode[18] and F: O(2) vibration[22]
538	536	536	530	529	527	529	531	A: Breathing of O(1) atoms†
			569	568		566		Unassigned
621	620	620	618	617		616		E: O(3) vibrations and weak Bi-O(1) and Bi-O(2) stretching

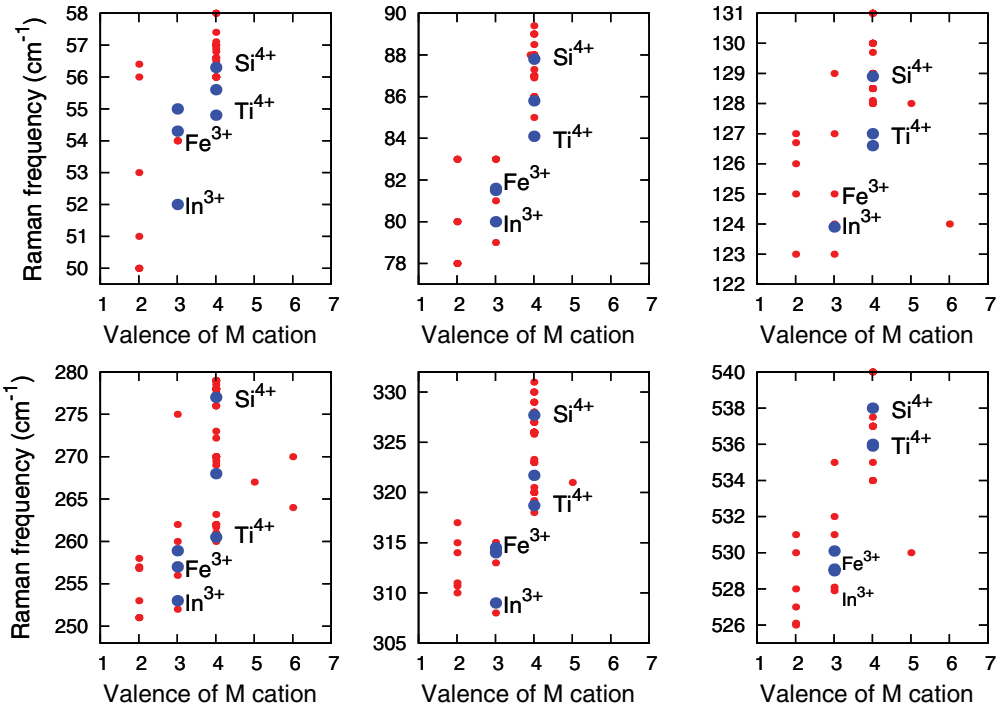

FIG. 5. (Color online) Frequency of the most pronounced Raman peaks for various compounds with different valences in their M cations. The big (blue) points correspond to the six samples synthesized in this study. (Si^{4+}, Ge^{4+}, Ti^{4+}, Ga^{3+}, Fe^{3+}, and In^{3+}). Bands from all Raman spectra found in the literature were also plotted (red).

The comparison in Fig. 5 shows that the force constants of the Bi-O framework are stronger for the tetravalent cations for all six modes. There are at least three possible explanations. One, the extra charge of the M cations accounts for higher force constants in the tetrahedra. However, since the modes plotted in Fig. 5 are mainly due to Bi-O force constants, then this does not seem to be the case. A second explanation is that the M^{4+} cations are able to fill all M positions, while for lower valences Bi^{3+} fills some of the M positions. However, there is not a significant difference in the frequencies of the compounds with +2 and +3 valences even though there should be more Bi^{3+} ions in the M position of the divalent compounds compared to the trivalent compounds. The final and more plausible explanation is that the higher valence cations have smaller ionic radii that fit better in the tetrahedron position.

2. *Ionic radius of the M cation*

Figure 6 shows the Raman frequencies of the compounds vs. the ionic radius of its M cation. The ionic radius was chosen based on a coordination number of 4. Complex compounds, such as $Bi_{36}MgP_2O_{60}$ and $Bi_{24}AlPO_{40}$, where the M site is shared by two elements with significantly different ionic radii, are not considered here. A decrease in frequency with increasing ionic radii is a clear trend displayed for all six modes. Across different sillenite compounds, there is no change in mass for the elements in the Bi-O framework; therefore the decrease in frequency must arise from a decrease of the force constants. This result shows that the ionic radius of the M cation has a strong effect on the Bi-O framework. It is expected that a large M cation pushes the O(3) atoms in the tetrahedron away but the effect is also strong enough to significantly push the O(1) and O(2) atoms outside the tetrahedron and increase the unit cell volume. As stated earlier, the comparison is shown for the results of different authors using different synthesis methods. We also synthesized $Bi_{12}SiO_{20}$, $Bi_{12}GeO_{20}$, $Bi_{12}TiO_{20}$, and $Bi_{25}GaO_{39}$ to rule out a systematic difference due to our preparation method. The mode frequencies of our samples agreed with those from other synthesis methods. In Fig. 6, the six big blue points correspond to our samples. (M = Si^{4+}, Ge^{4+}, Ti^{4+}, Ga^{3+}, Fe^{3+}, and In^{3+} in increasing ionic radii). The results show that the softening of the modes and decrease in force constants of the Bi-O framework is independent of the synthesis method.

3. *Effective crystal radius of the M site*

The stoichiometry presented by Valant *et al.* shows that the occupancy of the M site varies for different valences of the M cation. In pentavalent compounds, the M site is occupied 80% by the metal cation and 20% of the sites are vacant: $Bi_{12}(M^{5+}_{4/5}\,\square_{1/5})\,O_{20}$; while for tetravalent compounds the M site is occupied 100%: $Bi_{12}M^{4+}O_{20}$. Trivalent metal cations share half of the tetrahedral sites with Bi^{3+}: $Bi_{12}(Bi_{1/2}M^{3+}_{1/2})O_{19.5}$. And divalent compounds have two thirds of the M site occupied by bismuth: $Bi_{12}(Bi_{2/3}M^{2+}_{1/3})O_{19.33}$. In the last section, we showed that the cation in the tetrahedral site also affects the Bi-O framework outside the tetrahedron; therefore we should also consider the effect of Bi^{3+} in the M site. Bi^{3+} in a IV coordination is not presented on standard tables of ionic radii,[43] but we have extrapolated its IV ionic radius (0.89 Å) and crystal radius (1.03 Å) from higher coordination numbers. In Fig. 7, we used the crystal radius of the M cation and Bi^{3+}

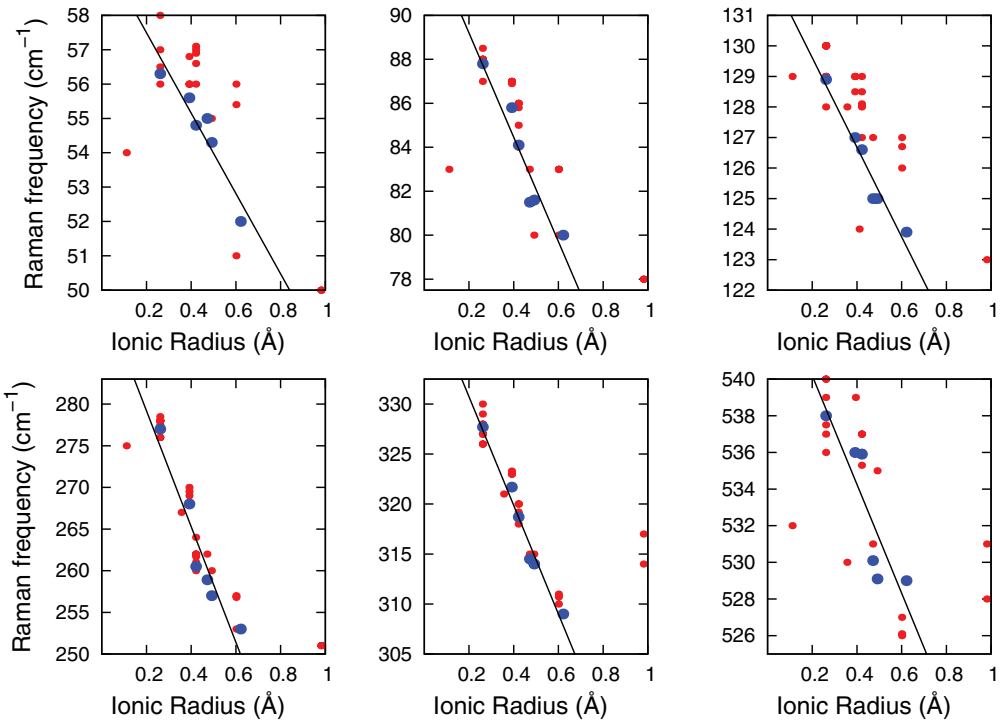

FIG. 6. (Color online) Frequency of the most pronounced Raman peaks vs the ionic radius of the M cation. The bands from all samples found in the literature were plotted. The data from our samples (blue), grown by the conventional solid state method, are shown as the bigger points. (Si^{4+}, Ge^{4+}, Ti^{4+}, Ga^{3+}, Fe^{3+}, and In^{3+} in increasing ionic radii). A line was fitted to our data. Notice that the majority of sillenites also follow the pattern of decreasing frequency vs increasing ionic radii.

to calculate the effective radius depending on the occupancy of Bi ions. This criterion yields a better agreement, compared to Fig. 6, for the large Pb^{2+} cation.

As a side note, it should be emphasized that the six vibrations mentioned belong to Bi and O vibrations and do not involve movement of the M cation. This assignment has been carried out by Mihailova using lattice dynamical calculations.[20,22] Therefore the patterns in frequency are not related to heavier M cations. Experimentally, the best piece of evidence is the spectra of $Bi_{12}GeO_{20}$ and $Bi_{12}TiO_{20}$. Ge is the heavier M cation yet its sillenite has consistently higher frequencies than the Ti sillenite; and this result is shown in spectra by different authors.[32,34] Also, Ga and Ge have similar masses and the germanium sillenite has significantly higher frequencies. The spectrum of the Ga^{3+} sillenite provides more evidence: If the large difference in frequencies between the In and Ge sillenite can be explained by the mass difference, then $Bi_{25}GaO_{39}$ should show splitting in the modes frequencies since half of the sites are occupied by the massive Bi^{3+} (heavier than In^{3+}) and the other half by Ga^{3+}. A small splitting is only observed for one of the modes (530 cm^{-1}) of the Ga sillenite and is missing in all others;[32] therefore, our spectra, and those found in the literature, support Mihailova's lattice dynamical calculations and mode assignments.[22]

D. Unit cell volume

The decrease in frequency across the compounds suggests an increasing unit cell volume: a symmetric expansion of the unit cell increases the average bond lengths and decreases the force constants. Figure 8 shows the frequencies of the modes versus the unit cell of the compound. The comparison is difficult due to some disagreements in the literature. Several authors report the lattice parameter of $Bi_{12}TiO_{20}$ around 10.188(6) Å,[44–46] while others report 10.175(2) Å.[47] Our result for the Ti sillenite, 10.177(2) Å, agrees with that from Valant *et al.*[47] The discrepancies are significant because they predict different patterns in increasing ionic radii versus unit cell volume (i.e., the unit cell volume of the Ti^{4+} sillenite would be larger than the Ga^{3+} and Fe^{3+} compounds). The discrepancies would give a very different pattern for Figure 8— the Ti compound would have a higher unit cell volume and higher center frequencies. The Fe^{3+} sillenite also has different reported values for the lattice parameter.[48–50] Our x-ray result for $Bi_{25}FeO_{39}$ [10.184(2) Å] agrees with Radaev *et al.*[50] and yields a larger unit cell volume for this compound than the Ti^{4+} and Ga^{3+} sillenite. Therefore our x-ray results on samples synthesized with the same methods show that the unit cell volume increases with larger M cation and the Raman spectra (see Fig. 8) also corroborate this pattern.

A larger unit cell for a larger M cation is physically reasonable: a large M cation pushes the O(3) in the tetrahedra and affects the oxygens in the Bi-O framework. This "pushing" effect from the tetrahedra to the Bi-O framework may have other effects such as distortion and inhomogeneous disorder. The section below examines the width of the Raman modes to compare the statistical distribution of force constants (related to bond lengths) for different compounds.

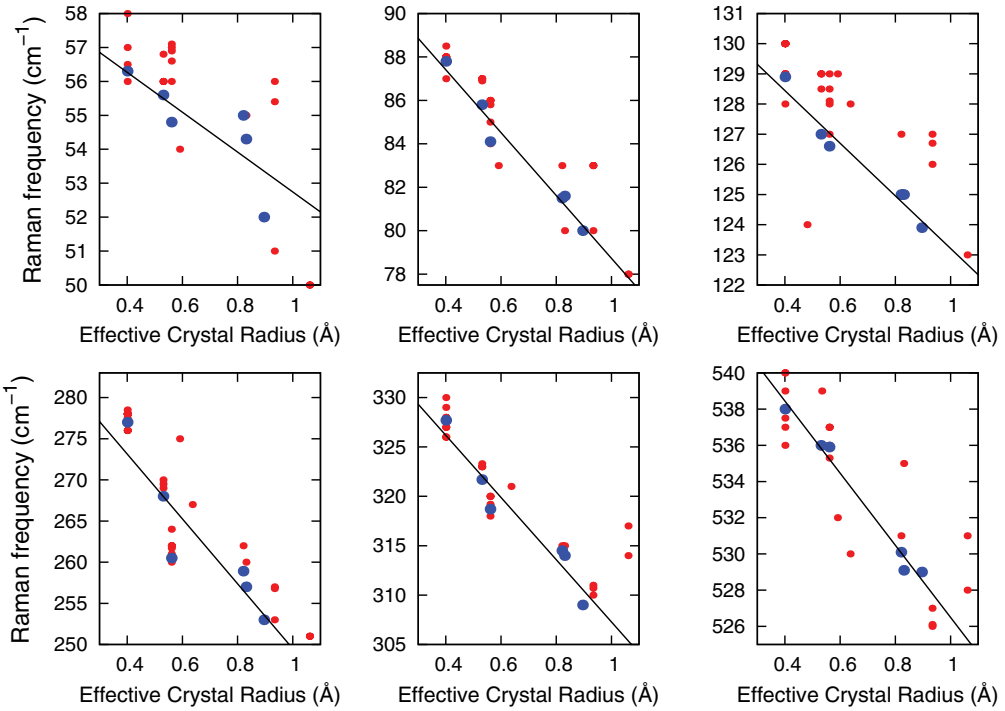

FIG. 7. (Color online) Frequency of the most pronounced Raman peaks vs the effective crystal radius of the M site.

E. Width of the modes

The Raman line widths in our spectra give indication of inhomogeneous disorder in the Bi-O framework. Figures 9 and 10 show the widths of the modes versus the ionic radius of the M cation and the effective crystal radius of the M site. The comparison shows that the Raman widths increase for larger ionic radii with a high jump from trivalent to tetravalent compounds. The larger Raman widths show higher standard deviations in the force constants for different unit cells. Since the force constants are related to the bond lengths, these six Raman modes give us a measurement of

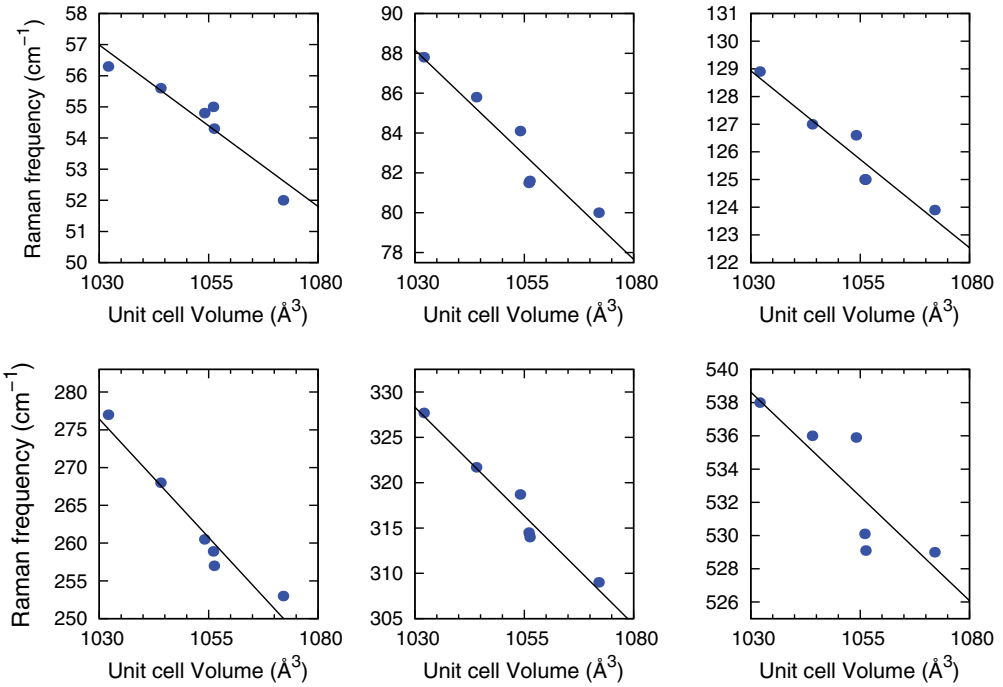

FIG. 8. (Color online) Frequency of the most pronounced Raman peaks vs the unit cell volume of the compound. As stated in the text, there are conflicting values for the lattice parameter of some compounds. The lattice parameter measured for our compounds are presented in this graph.

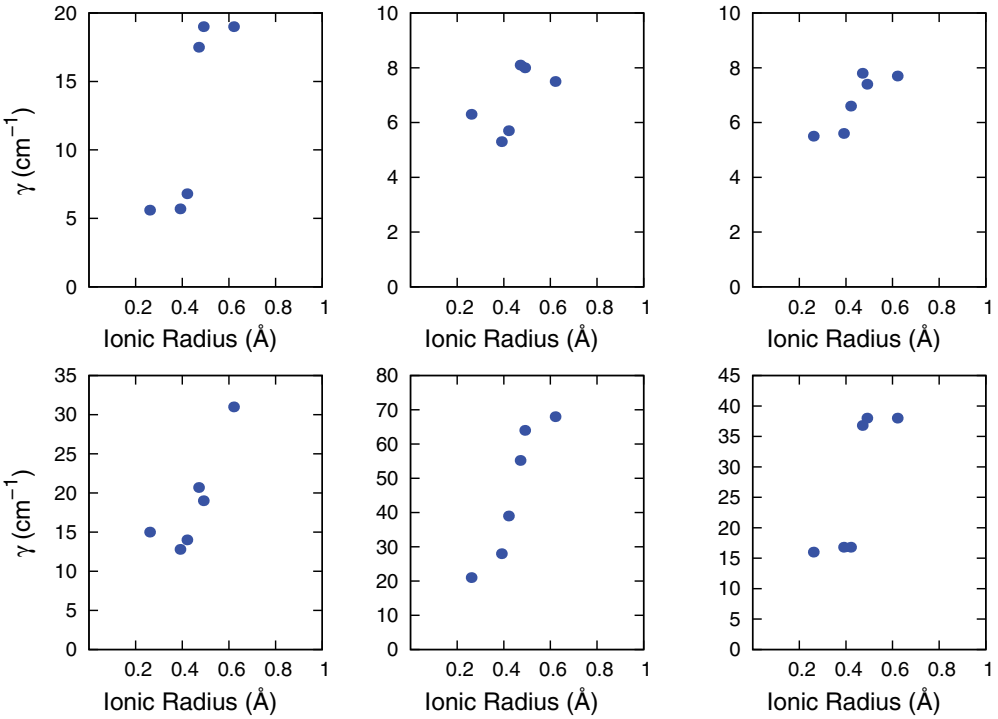

FIG. 9. (Color online) Width of the most pronounced peaks in the Raman spectra vs the ionic radius of its M cation. Very few papers report the width of the modes; only our six samples are shown.

the local deviations in Bi-O bond lengths across different unit cells. Differing bond lengths indicate random (x, y, z) displacements of the oxygens, or bismuth atoms, from their average positions. This inhomogeneous disorder may be caused by the larger M cation by distorting the tetrahedron and pushing into the Bi-O framework. Although this disorder in the long-range structure may be present in the XRD measurements, the effect may be negligible if only the oxygen atoms are randomly displaced from their average positions. X-ray measurements are dominated by the heavier elements (Bi) and small displacements of oxygens yield small deviations in the diffraction data. Also, the bismuth and O(1) sites already have very low symmetry and the displacements do not result in a lower symmetry site. Optics, however, is sensitive to the force constants of bonds to oxygen; therefore decreases of frequency and increases of widths give evidence of disorder.

In other compounds, Raman spectra can give additional evidence of disorder by detecting optically inactive modes of the ideal structure that appear due to disorder.[33,51] However, all vibrations are Raman active in the sillenite structure and we do not expect small deviations to produce new Raman-active modes. Also, unlike the displacement disorder in other compounds such as the pyrochlores, the displacements of O(1) and Bi atoms would not result in a lower symmetry site since these sites have very low symmetry to begin with.

It should also be noted that the evidence of distortion in the Bi-O framework is based on the previous computational and theoretical work that assigns these six vibrations to movement of the Bi, O(1) and O(2) atoms. We must also consider the possibility that these six vibrations are strong functions of the force constants of the M-O bonds of the tetrahedron and that these are significantly affected by the large M cations. Vacancies in the O(3) site and/or the partial occupancy of Bi^{3+} in the M site, as pointed out by Valant *et al.* would also contribute to this effect. Based on the literature, and the fact that six modes are studied, we conclude that the Bi-O framework is also affected. In summary, the Raman spectra results presented here show evidence of disorder and we hope may provide motivation for future synchrotron x-ray and neutron scattering measurements.

Finally, the widths of the 50 and 530 cm^{-1} modes are very sensitive to the valence of the M cation for it shows a large jump from the tetravalent compounds (Si, Ge, Ti) to the trivalent compounds (Ga, Fe, In). It would be interesting to synthesize pentavalent compounds, which should have small effective crystal radii, and analyze the width of the modes. The study would be useful in studying the valence of the Mn sillenite. In some studies Mn has been reported with a valence of +4,[36] while other authors have reported a valence of +5.[22]

F. The tetrahedral modes: 450 and 760 cm^{-1}

In an effort to understand the Raman spectra of sillenites, Ramdas[35] and Wojdowski[18] made an approximation where each MO_4 tetrahedron is isolated from the rest of the unit cell. This approximation is justified by the large mass of the bismuth atoms surrounding the tetrahedron. The heavy Bi atoms are compared to an infinitely massive wall that prevents the transfer of energy from the tetrahedron's vibration to the rest of the unit cell. The physical significance of both the 450 and 760 cm^{-1} modes is straightward. From Wadia's group theory

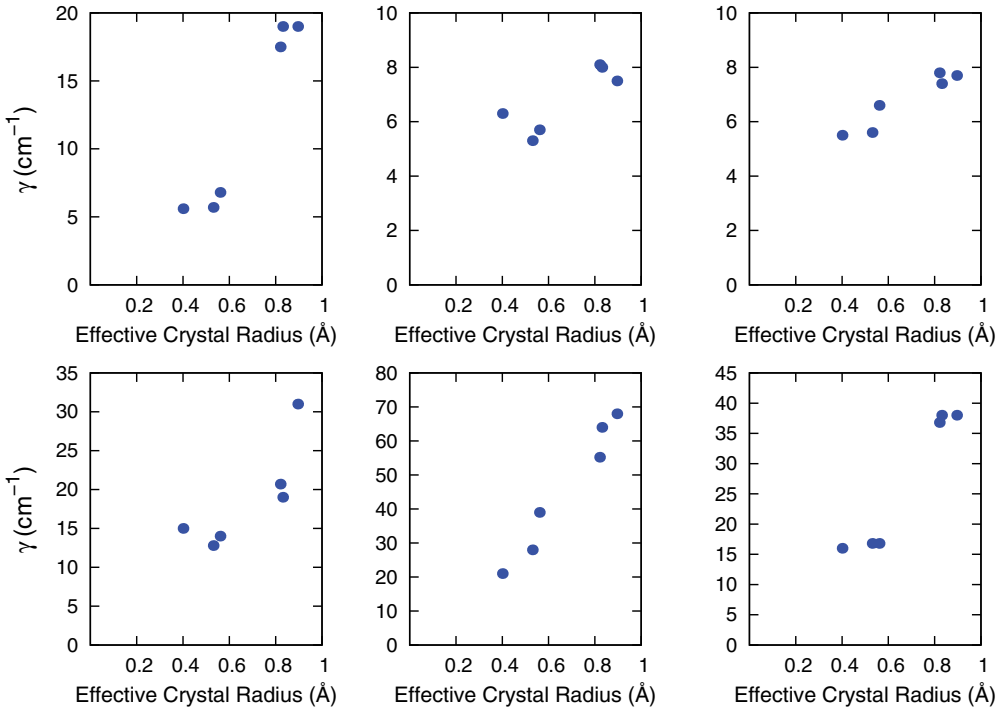

FIG. 10. (Color online) Width of the most pronounced peaks in the Raman spectra vs the effective crystal radius of the M site.

analysis of the isolated MO_4 tetrahedron; these two modes have *E* and *A* symmetries, respectively, but most importantly, only oxygen moves in these vibrations.[52] Therefore the frequency of these Raman modes should not depend on the mass of the M cation. Figure 11 has a similar comparison for the tetrahedral modes as the ones shown for the Bi-O framework modes. The 450 cm^{-1} mode shows that the strength of the force constants in the tetrahedron decrease with larger ionic radii. Unfortunately, there are fewer data points in the figure because not all the samples in the cited reports show this mode. Also, we should point out that the analysis of this mode is difficult because of the presence of an optically active *F* mode near this frequency due to a Bi-O bond not the tetrahedron.

The 760 cm^{-1} mode was observed in $Bi_{25}InO_{39}$ but not in $Bi_{25}FeO_{39}$. Bands in this high-frequency part of the spectrum correspond to either the symmetric or antisymmetric stretching mode of the MO_4 tetrahedra.[18,22] There is a general decrease in the mode frequency with larger ionic radii but there are few data points. In this region, weak bands may be confused with overtones and the analysis becomes more complicated. The absence of this mode has been used as proof that the tetrahedron does not behave as an isolated molecule.[32] However, Mn samples,[22] and other doped sillenites,[39,53] show a strong symmetric stretching mode and the intensity is attributed to a larger polarizability. In the IR spectra the 700–800 cm^{-1} modes tend to be stronger;[54,55] therefore future infrared measurements could corroborate the pattern seen in the 760 cm^{-1} Raman mode.

G. Relevance and future work

Our interpretation is that the evidence for the distortion of the Bi-O framework and the pattern closely followed by the sillenites is important for at least four reasons. First, Raman spectroscopy will be further useful in the study of new sillenites. We can predict the Raman frequencies of new sillenites using the proper valence and coordination IV ionic radius. In compounds where different authors have reached different conclusions regarding the valence of the M cation, such as the Mn sillenite,[19,22] Raman spectroscopy will offer additional evidence. Also, Raman spectroscopy could test different preparation methods. For example, the Raman spectra of $Bi_{12}SiO_{20}$ and $Bi_{12}TiO_{20}$ grown by mechanical alloying[56] show significantly lower frequencies than the frequencies for samples from other synthesis methods. Furthermore, the data suggests that increasing the milling time decreases the force constants in the Bi-O framework even further. Raman spectroscopy could also be used to study newly synthesized $Bi_{12}SiO_{20}$ thin-films grown by the sol-gel process.[57] Also, it is interesting that different groups have reported different lattice parameters for the $Bi_{12}TiO_{20}$ compound. Unfortunately, Raman measurements were not the purpose of those studies and we cannot compare them with our data. The reason for the differing lattice parameters in the literature is not the scope of this paper, but the strong patterns followed by our data (ionic radius, lattice parameter, mode width, mode center frequency) may be useful for future researchers synthesizing these compounds.

Second, the systematic decrease in Raman modes frequency versus the M ionic radius is an interesting test for first-principles calculations. Since the M cation inside the sillenite could be readily changed in first-principles calculations, it would be interesting to see if the relaxed structures show softer Raman modes in the Bi-O framework for larger M cations. Third, the wider Raman modes and decreased force constants of the Bi-O framework seem to originate from

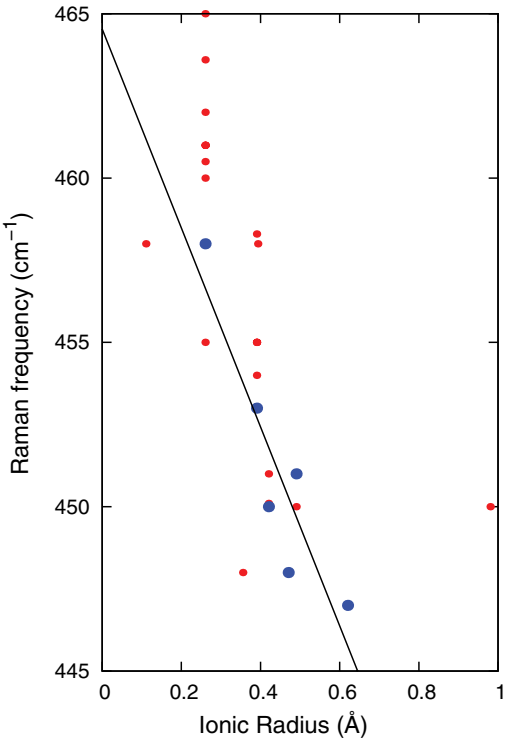

FIG. 11. (Color online) Comparison for the vibrational mode of the MO_4 tetrahedron. The blue points correspond to our samples grown by the conventional solid state method.

distortions caused by a large M cation. Similarly, the disorder in pyrochlores is caused by the lone pair of a large Bi atom,[58–62] and this disorder is considered an important factor in dielectric losses.[58] Although the possibility of displacement disorder is outside the scope of this work, it is indeed interesting to mention the possibility and stimulate further study of sillenites with large M ionic radii. And finally, fourth, a similar systematic study on the nonlinear properties of these materials could be compared to the Raman results and relate the contributions of the Bi-O framework to the nonlinear properties of these samples.

IV. CONCLUSIONS

$Bi_{25}InO_{39}$ and $Bi_{25}FeO_{39}$ have been synthesized by the conventional solid state method and the Raman spectra confirm that the samples were successfully prepared with the sillenite structure. The Raman modes were assigned to symmetry-allowed vibrations. Comparison across sillenites shows a robust relation between the ionic radii of the M cations and the frequency of the Raman modes in the Bi-O framework. The results show that large M cations decrease the force constants of the Bi-O framework and increase their deviation across unit cells. The increase in inhomogenous disorder is observed as the ionic radius and valence increase. Also, the clear relation between the Raman frequencies and the ionic radii of the M cation may be useful in the study of new sillenites and future first-principles calculations. Disorder in the Bi-O framework by large M cations may also be interesting for dielectric and nonlinear studies. The 450 cm^{-1} mode arising from vibrations in the tetrahedra also decreases for larger ionic radii M cations and directly shows a decrease in force constants. Future infrared work on these samples would be useful to study the vibrational modes arising from the tetrahedron.

ACKNOWLEDGMENTS

This work was supported in party by the National Science Foundation (NSF) Grants DMR-0805073, DMR-0958349, and the Office of Naval Research award N00014-06-1-0133. Also supported in part by a Grant-in-Aid from Japan Chemical Innovation Institute, and also by Adaptable and Seamless Technology Transfer Program through Target-driven R&D, Japan Science and Technology Agency. MWL acknowledges UNF for the Munoz fellowship.

[1] S. L. Sochava, K. Buse, and E. Krätzig, Phys. Rev. B **51**, 4684 (1995).
[2] H. C. Pedersen, D. J. Webb, and P. M. Johansen, J. Opt. Soc. Am. B **15**, 2573 (1998).
[3] V. Jerez, I. de Oliveira, and J. Frejlich, J. Appl. Phys. **109**, 024901 (2011).
[4] A. Ballman, H. Brown, P. Tien, and R. Martin, J. Cryst. Growth **20**, 251 (1973).
[5] V. Chmyrev, V. Skorikov, and E. Larina, Inorg. Mater. **42**, 381 (2006).
[6] A. Efremidis, N. Deliolanis, C. Manolikas, and E. Vanidhis, Appl. Phys. B **95**, 467 (2009).
[7] I. de Oliveira, T. dos Santos, J. Carvalho, and J. Frejlich, Appl. Phys. B **105**, 301 (2011).
[8] E. L. Venturini, E. G. Spencer, and A. A. Ballman, J. Appl. Phys. **40**, 1622 (1969).
[9] M. Peltier and F. Micheron, J. Appl. Phys. **48**, 3683 (1977).
[10] A. F. Lima, S. A. S. Farias, and M. V. Lalic, J. Appl. Phys. **110**, 083705 (2011).
[11] H. Deng, W. Hao, and H. Xu, Rare Metals **30**, 135 (2011).
[12] L. A. S. de Oliveira, J. P. Sinnecker, M. D. Vieira, and A. Pentón-Madrigal, J. Appl. Phys. **107**, 09D907 (2010).
[13] R. Rao, A. B. Garg, and T. Sakuntala, J. Appl. Phys. **108**, 083508 (2010).
[14] L. Wiehl, A. Friedrich, E. Haussühl, W. Morgenroth, A. Grzechnik, K. Friese, B. Winkler, K. Refson, and V. Milman, J. Phys.: Condens. Matter **22**, 505401 (2010).
[15] V. Marinova, M. Veleva, D. Petrova, I. M. Kourmoulis, D. G. Papazoglou, A. G. Apostolidis, E. D. Vanidhis, and N. C. Deliolanis, J. Appl. Phys. **89**, 2686 (2001).
[16] M. Valant and D. Suvorov, J. Am. Ceram. Soc. **85**, 355 (2002).
[17] V. Marinova, S. Lin, and K. Hsu, Opt. Memory Neural Network. **20**, 7 (2011).
[18] W. Wojdowski, Phys. Status Solidi B **130**, 121 (1985).

[19]M. Valant and D. Suvorov, Chem. Mater. **14**, 3471 (2002).
[20]B. Mihailova, G. Bogachev, V. Marinova, and L. Konstantinov, J. Phys. Chem. Solids **60**, 1829 (1999).
[21]S. Neov, V. Marinova, M. Reehuis, and R. Sonntag, Appl. Phys. A **74**, s1016 (2002).
[22]B. Mihailova, M. Gospodinov, and L. Konstantinov, J. Phys. Chem. Solids **60**, 1821 (1999).
[23]F. D. Hardcastle, I. E. Wachs, H. Eckert, and D. A. Jefferson, J. Solid State Chem. **90**, 194 (1991).
[24]H. Franklin and W. Israel, J. Phys. Chem. **95**, 10763 (1991).
[25]H. F. D. and W. I. E., J. Raman Spectrosc. **26**, 407 (1995).
[26]N. Sammes, G. Tompsett, and A. Cartner, J. Mater. Sci. **30**, 4299 (1995).
[27]A. Egorysheva, V. Burkov, Y. Kargin, V. Plotnichenko, and V. Koltashev, Crystallogr. Rep. **50**, 127 (2005).
[28]A. Salazar-Pérez, M. Camacho-López, R. Morales-Luckie, V. Sánchez-Mendieta, F. Ureña-Núñez, and J. Arenas-Alatorre, Superficies y Vacío **18**, 4 (2005).
[29]J. Alonso, R. Diamant, E. Haro-Poniatowski, M. Fernández-Guasti, G. Muñoz, I. Camarillo, M. Jouanne, and J. Morhange, Appl. Surf. Sci. **109-110**, 359 (1997).
[30]H. Sekhar, P. P. Kiran, and D. N. Rao, Mater. Chem. Phys. **130**, 113 (2011).
[31]D. J. Dunstan and M. D. Frogley, Rev. Sci. Instrum. **73**, 3742 (2002).
[32]R. J. Betsch and W. B. White, Spectrochim. Acta, Part A **34**, 505 (1978).
[33]D. J. Arenas, L. V. Gasparov, W. Qiu, J. C. Nino, C. H. Patterson, and D. B. Tanner, Phys. Rev. B **82**, 214302 (2010).
[34]A. Egorysheva, V. Burkov, V. Gorelik, Y. Kargin, and A. Chervyakov, Crystallogr. Rep. **46**, 461 (2001).
[35]S. Venugopalan and A. K. Ramdas, Phys. Rev. B **5**, 4065 (1972).
[36]U. Delicat, S. Radaev, M. Trömel, P. Behrens, Y. Kargin, and A. Mar'in, J. Solid State Chem. **110**, 66 (1994).
[37]Y. G. Zaretskii, G. Kurbatov, V. V. Prokofev, Y. I. Ukhanov, and Y. V. Shmartsev, Opt. Spectrosc. **54**, 569 (1983).
[38]E. S. M, Phys. Status Solidi A **123**, K105 (1984).
[39]B. Mihailova, L. Konstantinov, D. Petrova, and M. Gospodinov, Solid State Commun. **102**, 441 (1997).
[40]L. Escobar-Alarcón, E. Haro-Poniatowski, M. Fernández-Guasti, A. Perea, C. Afonso, and T. Falcón, Appl. Phys. A **69**, S949 (1999).
[41]G. Avdeev, T. Milenov, A. Egorysheva, K. Petrov, V. Skorikov, R. Titorenkova, and P. Rafailov, Russ. J. Inorg. Chem. **56**, 913 (2011).
[42]A. Egorysheva, T. Milenov, P. Rafailov, C. Thomsen, R. Petrova, V. Skorikov, and M. Gospodinov, Solid State Commun. **149**, 1616 (2009).
[43]R. D. Shannon and C. T. Prewitt, Acta Crystallogr. Sect. B **25**, 925 (1969).
[44]V. Radaev and S. F. Simonov, Kristallografiya **37**, 914 (1992).
[45]D. C. N. Swindells and J. L. Gonzalez, Acta Crystallogr. Sect. B **44**, 12 (1988).
[46]S. M. Efendiev, T. Z. Kulieva, V. A. Lomonov, M. I. Chiragov, M. Grandolfo, and P. Vecchia, Phys. Status Solidi A **74**, K17 (1982).
[47]M. Valant and D. Suvorov, J. Am. Ceram. Soc. **84**, 2900 (2001).
[48]D. Craig and N. Stephenson, J. Solid State Chem. **15**, 1 (1975).
[49]S. Phapale, R. Mishra, and D. Das, J. Nucl. Mater. **373**, 137 (2008).
[50]S. F. Radaev, L. A. Muradyan, and V. I. Simonov, Acta Crystallogr. Sec. B **47**, 1 (1991).
[51]K. H. Miller, P. W. Stephens, C. Martin, H. Berger, G. L. Carr, and D. B. Tanner, arXiv:1206.1610v1.
[52]W. Wadia, Phys. Chem. Glass. **9**, 115 (1968).
[53] V and Marinova, Opt. Mater. **15**, 149 (2000).
[54]D. Senuliene, G. Babonas, E. I. Leonov, I. Muminov, and V. M. Orlov, Phys. Status Solidi A **84**, 113 (1984).
[55]W. Wojdowski, Phys. Status Solidi B **123**, K101 (1985).
[56]I. F. Vasconcelos, M. A. Pimenta, and A. S. B. Sombra, J. Mater. Sci. **36**, 587 (2001).
[57]A. Veber, Špela Kunej, and D. Suvorov, Ceram. Int. **36**, 245 (2010).
[58]S. Kamba, V. Porokhonskyy, A. Pashkin, V. Bovtun, J. Petzelt, J. C. Nino, S. Trolier-McKinstry, M. T. Lanagan, and C. A. Randall, Phys. Rev. B **66**, 054106 (2002).
[59]M. Chen, D. B. Tanner, and J. C. Nino, Phys. Rev. B **72**, 054303 (2005).
[60]B. Melot, E. Rodriguez, T. Proffen, M. Hayward, and R. Seshadri, Mater. Res. Bull. **41**, 961 (2006), Special Issue Dedicated to Professor Gerard Ferey.
[61]C. H. Patterson, Phys. Rev. B **82**, 155103 (2010).
[62]G. S. Babu, M. Valant, K. Page, A. Llobet, T. Kolodiazhnyi, and A.-K. Axelsson, Chem. Mater. **23**, 2619 (2011).